https://doi.org/10.5194/wcd-2021-5
Preprint. Discussion started: 27 January 2021

Weather and Climate Dynamics Discussions
Open Access
EGU

Linking air stagnation in Europe with the large-scale atmospheric circulation

Jacob W. Maddison[1], Marta Abalos[1], David Barriopedro[2], Ricardo García-Herrera[1,2], Jose M. Garrido-Perez[1], and Carlos Ordóñez[1]

[1]Department of Earth Physics and Astrophysics, Universidad Complutense de Madrid, Madrid, Spain
[2]Instituto de Geociencias (IGEO), CSIC-UCM, Madrid, Spain

Correspondence: Jacob Maddison (JACOBMAD@ucm.es)

Abstract. The build-up of pollutants to harmful levels can occur when meteorological conditions favour their production or accumulation near the surface. Previous studies have shown that such conditions are often associated with air stagnation. Understanding the development of stagnant conditions is therefore crucial for studying poor air quality. The link between European air stagnation and the large-scale circulation is investigated in this article across all seasons and the 1979–2018 period. Dynamical based indices identifying atmospheric blocking, Rossby wave breaking, subtropical ridges, and the North Atlantic eddy-driven and subtropical jets are used to describe the large-scale circulation as predictors in a statistical model of air stagnation variability. It is found that the large-scale circulation can explain approximately 60% of the variance in monthly air stagnation in five distinct regions within Europe. The variance explained by the model does not vary strongly across regions and seasons. However, the dynamical indices most related to air stagnation do depend on region and season. The blocking and Rossby wave breaking predictors tend to be the most important for describing air stagnation variability in northern regions whereas ridges and the subtropical jet are more important to the south. The demonstrated correspondence between air stagnation and the large-scale circulation can be used to assess the representation of stagnation in climate models, which is key for understanding how air quality and its associated health risks may change in the future.

1 Introduction

Poor air quality poses one of the largest environmental threats to public health. Long term exposure to air pollutants such as particulate matter (PM) and ozone can cause severe cardiovascular and respiratory diseases and is responsible for between two and four hundred thousand premature deaths every year in Europe (World Health Organization, 2011; Giannadaki et al., 2016; European Environment Agency, 2020). Risks depend strongly on the weather, increasing when meteorological conditions favour the production or accumulation of the pollutants in the lowest part of the atmosphere (Ordóñez et al., 2005; Jacob and Winner, 2009; Weaver et al., 2009; Barmpadimos et al., 2011; Dawson et al., 2014). It is therefore key to characterize such favourable conditions, often referred to as *air stagnation*. Furthermore, climate change is expected to increase the occurrence of air stagnation (Mickley et al., 2004; Leung and Gustafson Jr, 2005; Horton et al., 2012, 2014; Caserini et al., 2017; Gao et al., 2020; Lee et al., 2020), which can result in increased pollutant levels (Weaver et al., 2009; Jacob and Winner, 2009)

https://doi.org/10.5194/wcd-2021-5
Preprint. Discussion started: 27 January 2021

Weather and Climate Dynamics Discussions
Open Access
EGU

and emphasises the need to fully understand air stagnation occurrence and its variability. Most studies have mainly focused on local conditions when describing air stagnation, without considering synoptic-scale structures and large-scale features of the atmospheric circulation. In this article, we use the large-scale atmospheric circulation to describe the variability of air stagnation within distinct regions of Europe.

Air stagnation refers to a period when a stable air mass becomes settled over a region and remains quasi-stationary for an extended amount of time. Weak winds in the lower to mid-troposphere and an absence of precipitation during air stagnation prohibit the ventilation and washout of particles so pollutants can accumulate near the surface. Regions in the tropics generally experience highest air stagnation frequencies (Horton et al., 2012, 2014), though several regions in the midlatitudes, such as North America, China and the Mediterranean, have stagnation frequencies over 40% (e.g., Horton et al., 2012, 2014; Huang et al., 2017; Garrido-Perez et al., 2018). Air stagnation has been shown to increase concentrations of ozone and PM in Europe (Garrido-Perez et al., 2018), cities in Asia (Wang et al., 2016; Zhang et al., 2016; Liao et al., 2018; Kanawade et al., 2020), and in North America (Valente et al., 1998; Schnell and Prather, 2017; Sun et al., 2017). Air stagnation events have been identified in reanalysis or model data sets using multiple criteria based on local weather conditions. Commonly used air stagnation indices (ASIs) include terms based on the wind speed at 10 m (Wang and Angell, 1999; Horton et al., 2012; Wang et al., 2016, 2018), wind speed in the boundary layer (Huang et al., 2018), boundary layer height (Wang et al., 2016, 2018) and precipitation (Wang and Angell, 1999; Horton et al., 2012; Wang et al., 2016, 2018; Huang et al., 2018). However, similar local weather conditions can occur under very different rearrangements of the large-scale flow. Therefore, there is a need to bridge the gap between local air stagnation and large-scale atmospheric circulation.

The large-scale flow is inherently related to air stagnation occurrence in Europe and thus also to air quality. Their relation can be summarised by considering the dynamics of midlatitude weather. The North Atlantic jet streams and Rossby waves are the main drivers of midlatitude weather, and are associated with high-impact weather systems such as atmospheric blocking and extratropical cyclones, which exert a strong control over surface conditions (Hoskins et al., 1985). Blocking events typically occur when a large-scale ridge in an upper-level Rossby wave develops (e.g. Woollings et al., 2018). They are an obvious candidate for driving air stagnation events as they are characterised by a synoptic-scale, quasi-stationary anticyclone (Rex, 1950), and thus provide the weak winds and absence of precipitation that define air stagnation. Blocks have been shown to increase pollutant levels in Europe (Hamburger et al., 2011; Garrido-Perez et al., 2017; Ordoñez et al., 2017; Webber et al., 2017; Vautard et al., 2018), the United States (Comrie and Yarnal, 1992), and in Asia (Yun and Yoo, 2019). The position of the North Atlantic jet stream (Ordóñez et al., 2019), the presence of subtropical ridges (Garrido-Perez et al., 2017; Ordoñez et al., 2017), and the passage of midlatitude cyclones (Leibensperger et al., 2008; Tai et al., 2010, 2012; Leung et al., 2018) can also influence air stagnation development. A comprehensive study linking European air stagnation occurring throughout the year with such dynamical features is presented here for the first time.

Air stagnation in different regions in Europe exhibits distinct spatial characteristics. Regions in the south of Europe experience frequent stagnation whilst the frequency and temporal variability of stagnation is generally lower in northern regions (Horton et al., 2012, 2014; Garrido-Perez et al., 2018). A comparison of three popular ASIs for Europe was recently performed by Garrido-Perez et al. (2021). Whilst describing the conditions necessary for air stagnation is intuitively straight forward,

https://doi.org/10.5194/wcd-2021-5
Preprint. Discussion started: 27 January 2021

objectively identifying stagnant conditions from observational or model data can be more complicated as it usually relies on indices based on predetermined, arbitrary thresholds of meteorological variables that characterise stagnation (e.g. Wang and Angell, 1999; Horton et al., 2012, 2014; Wang et al., 2016, 2018; Huang et al., 2017). Garrido-Perez et al. (2021) showed that despite the frequency of stagnation being similar across the indices, differences in the indices' seasonal cycle and effect on pollutant build up are evident and means results obtained using a single ASI should be taken with caution because they might be sensitive to the ASI used.

With this in mind, the aims of this study are (i) to complete a comprehensive identification and comparison of the large-scale drivers of air stagnation within Europe, (ii) to quantify the amount of monthly variability in air stagnation that can be explained by the large-scale circulation, and (iii) to assess the sensitivity of the results to the air stagnation index.

The article is presented as follows. Section 2 contains a description of the data, the various circulation indices used throughout the article and the statistical model used. The large-scale circulation patterns identified during air stagnation are discussed in section 3. In section 4, the statistical model is analysed, its results explained in detail for a specific case and then used to compare three different air stagnation indices. The article is concluded in Section 5.

2 Data and methods

Several indices are used in this study to identify both air stagnation and relevant dynamical features. A brief description of each index is included but the reader is referred to the referenced papers for further information. All data used in this study is from the European Centre for Medium Range Weather Forecasts' ERA5 reanalysis (Hersbach et al., 2020). Data is interpolated onto a one degree grid for the analysis and covers the period 1979–2018, and the North Atlantic and European region (100°W – 80°E, 20–85° N).

2.1 Air stagnation indices

The ASI introduced in Horton et al. (2012) is used for most of the analyses presented in this study. A grid point is defined as stagnant if: (i) the daily mean wind speed at 10 m is less than 3.2 m/s, (ii) the daily mean wind speed at 500 hPa is less than 13.0 m/s, and (iii) total daily precipitation is less than 1 mm (a dry day). Values at 0000, 0600, 1200 and 1800 UTC are averaged to calculate the daily mean wind speeds and hourly precipitation totals are summed to calculate the daily precipitation. We compare our findings with two other ASIs to ensure the robustness of their results.

The ASI by Wang et al. (2016, 2018) defines stagnation when precipitation is below 1 mm and the boundary layer height is below a certain threshold. The threshold is a function of season and wind speed at 10 m (see Wang et al. (2018) for further details). Huang et al. (2018) use an ASI that again requires daily precipitation less than 1 mm. For stagnation, it is also required that the vertical integral of the horizontal wind speed within the boundary layer is less than 6000 m^2/s, and that there is no potential thunderstorm activity on that day. Thunderstorm activity is ruled out by excluding days with CAPE > 100 J/kg and CIN > − 50 J/kg. These values have been modified for European stagnation following Taszarek et al. (2018) and Garrido-Perez et al. (2021).

https://doi.org/10.5194/wcd-2021-5
Preprint. Discussion started: 27 January 2021

Weather and Climate Dynamics Discussions
Open Access
EGU

2.2 Dynamical indices

To link the large-scale circulation to air stagnation we use several daily dynamical indices that describe key features of the extratropical flow. Blocking, Rossby wave breaking (RWB), subtropical ridges, and the latitude and speed of the eddy-driven and subtropical North Atlantic jets are identified using indices based on various meteorological variables. These features of the large-scale circulation do not represent the full spectrum of synoptic systems that characterize the midlatitude atmospheric circulation, but are chosen because of their known association with air stagnation (section 1).

Atmospheric blocking is identified using the index of Scherrer et al. (2006). A block is identified using instantaneous meridional gradients in geopotential height at 500 hPa ($Z500$) (at 1200 UTC). The method looks for the overturning of the geopotential height contours in the midlatitudes (between 35 and 75°N) characteristic of a block and defines a grid point as blocked when the gradient from the south is positive and the gradient to the north is strongly negative (less than -10 m/degree). A persistence criteria of 3 days is used to identify block events.

RWB is calculated following the definition of Masato et al. (2012). Using the daily average potential temperature field on the dynamical tropopause (potential vorticity surface at 2 PVU, θ_{2PVU}), RWB is identified when the meridional gradient of potential temperature is reversed. Although RWB often occurs in association with blocking, these events are typically persistent. By not imposing persistence criteria, we also account for transient RWB events, including those associated with cyclone development (e.g. Gómara et al., 2014). In addition, RWB captures persistent flow reversals dominated by cyclonic wave breaking that may be missed by the blocking index, which is known to be biased towards anticyclonic blocks and can miss some omega type blocks (Barriopedro et al., 2010).

Subtropical ridges are classified following a slightly modified method of that developed by Sousa et al. (2018). Ridges are defined as positive $Z500$ anomalies in the subtropical midlatitudes (south of 50°N in all seasons except summer when 55°N is used) that do not extend futher poleward. The local 60th percentile of the daily $Z500$ series (smoothed with a 31-day running mean) is employed to identify positive anomalies. A ridge is then identified when more than half of the subtropical midlatitude grid points but less than half of the northern midlatitude grid points are above their 60th percentile in three separate longitudinal sectors (Atlantic, ATL, 30°W–0°, European, EUR, 0°–30°E, and Russian, RUS, 30°E–60°E). These criteria are chosen to avoid double counting blocks (i.e. to ensure blocks are not detected as subtropical ridges). The less strict thresholds for identifying ridges were chosen to increase the frequency of ridges, therefore providing a more balanced frequency of events (as compared with blocking and RWB), which in turn is expected to yield more robust linkages in the statistical model.

The *eddy-driven jet speed* and *latitude* are calculated using the index introduced in Woollings et al. (2010). The daily mean zonal wind is averaged vertically (every 75 hPa between 925 and 700 hPa) and zonally (between 0 and 60°W). A 10-day smoothing is then applied to remove the influence of individual synoptic systems. The magnitude and latitude of the maximum wind speed of the resulting meridional profile are selected as the eddy-driven jet speed and latitude, respectively.

The *subtropical jet speed* and *latitude* are described using the zonal wind at 250 and 200 hPa. Following the method used to describe the eddy-driven jet, the daily mean zonal wind is averaged vertically (between 250 and 200 hPa) and zonally (between 20°E and 60°W) and then low-pass filtered. The magnitude and latitude of the maximum wind speed of the resulting

https://doi.org/10.5194/wcd-2021-5
Preprint. Discussion started: 27 January 2021

Weather and Climate Dynamics Discussions
Open Access
EGU

meridional profile are selected as the subtropical jet speed and latitude, respectively. The eddy-driven and subtropical jet can at times be indistinguishable, particularly in summer, but in many cases they are expected to be separated (as inferred from the climatological means: see also Molnos et al. (e.g. 2017)). Furthermore, the eddy-driven jet speed and upper-level wind speed will likely more strongly influence the lower- and upper-level wind criteria of the ASI, respectively.

Together, these dynamical indices provide a comprehensive picture of the large-scale circulation over Europe. We construct a multiple linear regression (MLR) model with these indices as predictors of the variability in air stagnation. Blocks, RWB and ridges are referred to as regional predictors as they are identified within each region, whilst the eddy-driven and subtropical jet are called large-scale (or Europe-wide) as they are defined in areas covering more than one of the regions. Using all of the predictors ensures we include major factors that are favourable for air stagnation but means that they aren't necessarily independent. For example, the blocking and Rossby wave breaking indices or the eddy-driven and subtropical jet indices may at certain times identify the same large-scale feature. Their collinearity and relative importance for stagnation will be taken into account by the MLR model, as described in the next section.

2.3 Stepwise multiple linear regression

MLR models are used to study the linear relationship between a chosen response variable and a set of predictor variables. Here we use the monthly series of air stagnation and the set of dynamical indices as the response and predictor variables, respectively. The MLR model thus takes the form

$$ASI = \beta_0 + \beta_1 I_1 + \beta_2 I_2 + ... + \beta_k I_k, \quad (1)$$

where ASI is the air stagnation time series, each I represents a dynamical index, β_0 is the model intercept and the remaining β terms are the regression coefficients. The regression coefficients are estimated using a least-squares approach (Montgomery et al., 2012). This regression analysis is applied to model the monthly variability of stagnation for separate regions and seasons, as described in Section 4.

A stepwise approach has been used to select the dynamical indices that account for the largest variance of air stagnation from the total set of predictors. Stepwise approaches have been used to model the variability of pollutants in Europe (Barmpadimos et al., 2011, 2012; Otero et al., 2016; Garrido-Perez et al., 2021). The goal of the stepwise approach is to inform which of the predictors can be excluded from the MLR model without losing a significant amount of the variance explained by the model. The method consists of five steps. **(i)** A linear model for air stagnation is constructed for each of the dynamical indices separately and the index providing the most skill (highest R^2) is selected. **(ii)** The remaining indices are added one at a time to construct MLR models with an additional predictor. The added index that yields the most skilful model is selected. **(iii)** The choice from step (i) is verified. We remove the first variable from the model and construct models with the variable selected from step (ii) and each of the remaining variables separately. If any of the new models have a higher R^2 than that constructed in step (ii), the new variables replace those previously selected, else those from step (ii) remain. **(iv)** Collinearity between variables is checked. The linear correlation between the indices selected at each step is used to calculate the Variance Inflation Factor (Freund et al., 1998). If this exceeds a threshold (here chosen to be 5.0), indicating the predictors are highly correlated,

https://doi.org/10.5194/wcd-2021-5
Preprint. Discussion started: 27 January 2021

the variable adding least skill to the model is removed. **(v)** Steps (ii) to (iv) are repeated until the addition of a predictor increases the explained variance by less than 1% or until all the predictors have been included already.

3 The large-scale circulation during air stagnation

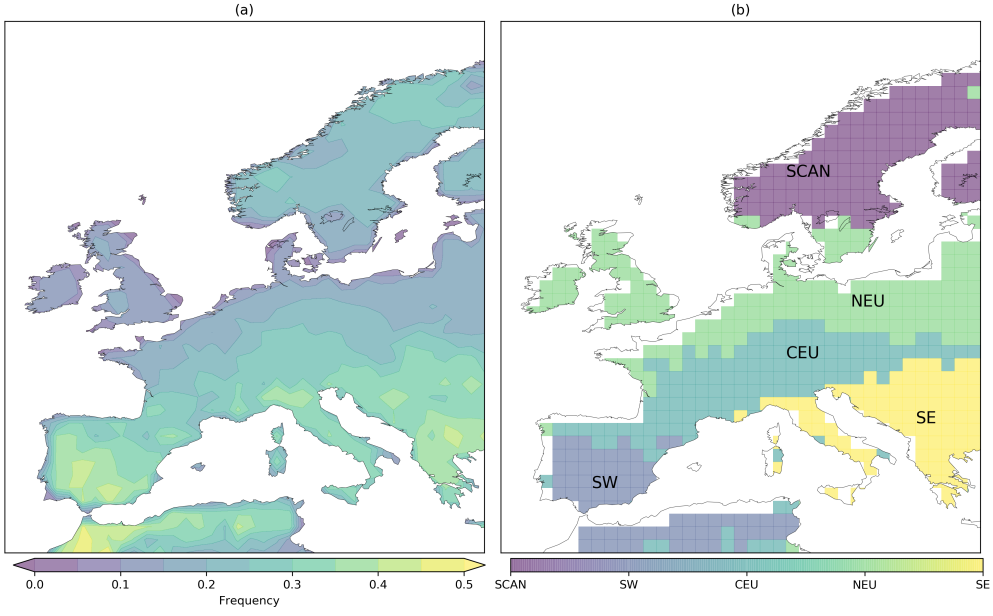

Figure 1. (a) The annual of frequency of air stagnation in Europe between 1979 and 2018 in the ERA5 data set. (b) Regions within Europe identified as having distinct air stagnation characteristics. These regions have been named Scandinavia (SCAN), northern Europe (NEU), central Europe (CEU), southwest Europe (SW) and southeast Europe (SE), following Garrido-Perez et al. (2018).

The climatological frequency of air stagnation in the ERA5 dataset is shown in Figure 1. In Europe, air stagnation is most common in the Mediterranean region (plus northern Africa) with annual stagnation frequencies in the region around 40%. Frequencies then reduce polewards (values of 15% for the UK and across north-central Europe) before increasing again in Scandinavia where stagnation frequency is near 30%. Five regions within Europe with distinct air stagnation characteristics were identified by clustering the monthly frequencies of air stagnation as inGarrido-Perez et al. (2018): Scandinavia (SCAN), northern Europe (NEU), central Europe (CEU), southwest Europe (SW) and southeast Europe (SE). The regions are depicted in Figure 1 (b).

https://doi.org/10.5194/wcd-2021-5
Preprint. Discussion started: 27 January 2021

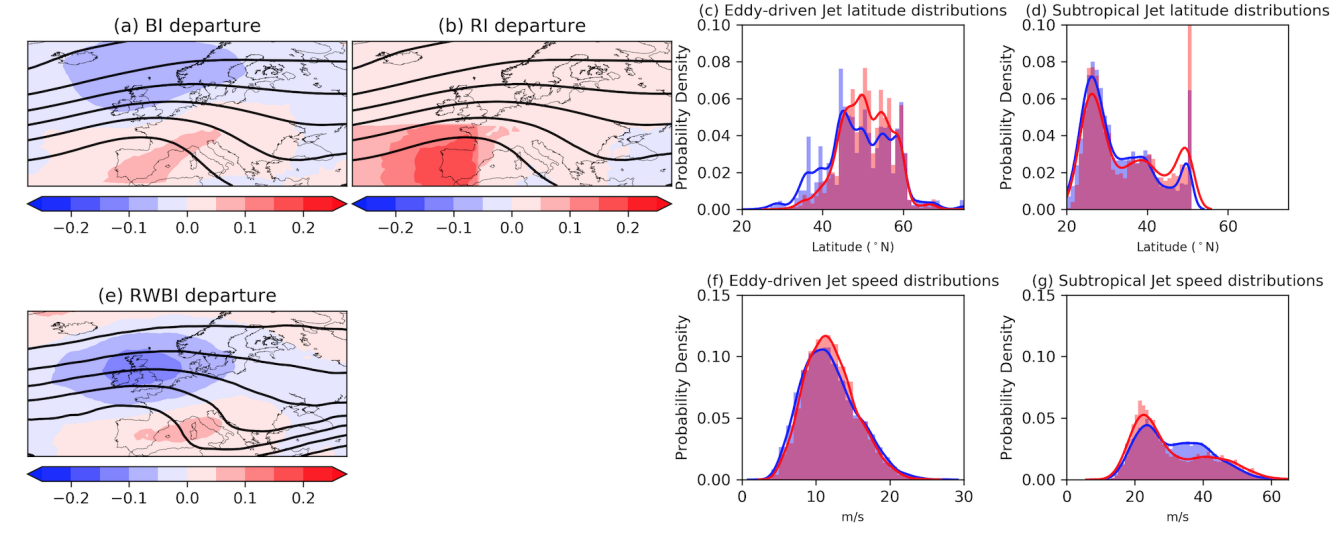

Figure 2. Composites of the (a) blocking index (shading) and Z500 (line contours), (b) ridge index (shading) and Z500 (line contours), and (e) Rossby wave breaking index (shading) and θ_{2PVU} (line contours) for stagnant days over SW. In (a), (b) and (e) the blocking, ridge and Rossby wave breaking index frequencies are presented as departures from their annual climatological frequencies, respectively. (c) The climatological annual eddy-driven jet stream latitude distribution (blue) and jet latitude distribution during stagnant days (red). (f) As in (c) but for the speed of the eddy-driven jet stream. (d) The climatological annual subtropical jet stream latitude distribution (blue) and that during stagnation (red). (g) As in (d) but or the subtropical jet speed. Data source: ERA5 reanalysis during 1979-2018.

3.1 Annual air stagnation events

In this section, composites of the large-scale circulation are shown for air stagnation events occurring in selected regions. Air stagnation events are defined as occasions when stagnation occurs in at least half of the grid points within a region for at least four consecutive days. A threshold of four days was also used to define stagnation events in Wang and Angell (1999) and Huang et al. (2017). Composites are shown for two regions, SW and NEU, as examples of the distinct effect of the large-scale circulation on stagnation in Southern and Northern Europe. Note that in the case of subtropical ridges, the algorithm described in Section 2.2 detects them in three longitudinal sectors (ATL, EUR and RUS). In the following, they will be considered over the three stagnation regions where they may be found (SW, CEU and SE), because by definition they do not extend northward to cover NEU and SCAN.

Annual mean composites of the large-scale circulation for air stagnation events in SW are shown in Figure 2. When stagnation occurs in SW, there is often a subtropical ridge extending into southwestern Europe. This is evidenced by an ∼20% increase in the climatological frequency of subtropical ridging over the region (Fig. 2 (b)). The ridging pattern present in the composite $Z500$ field (Fig. 2 (a), (b)) can sometimes exhibit a flow reversal in midlatitudes, resulting in a slight increase in block frequency over the region. Rossby wave breaking is less frequent to the north of SW during stagnation, consistent with

https://doi.org/10.5194/wcd-2021-5
Preprint. Discussion started: 27 January 2021

the upper-level jet being centred over this region. Both jets are more frequently observed around 50°N during stagnation, which likely reflects that the two can merge north of the SW region. Specifically, the eddy-driven jet is less frequently in its southern mode during SW stagnation (red distribution in Fig. 2(c)) and tends to be located further north. The subtropical jet latitude distribution during stagnation is more similar to its climatology, with only a slight increase in its northern flank and decrease in its southern latitudes. The speed of the eddy-driven jet is increased when stagnation occurs in SW, which is a robust feature associated with subtropical ridges (Sousa et al., 2018), while the subtropical jet speed is reduced. Note that the intensification and weakening of the eddy-driven and subtropical jets, respectively, occur at different latitudes and longitudinal sectors. The stagnation speed and latitude distributions of both jets are significantly different from their climatologies ($p<0.01$). The composites of each dynamical index are similar for SE stagnation, but with the increased frequency of ridges shifted to the east (not shown).

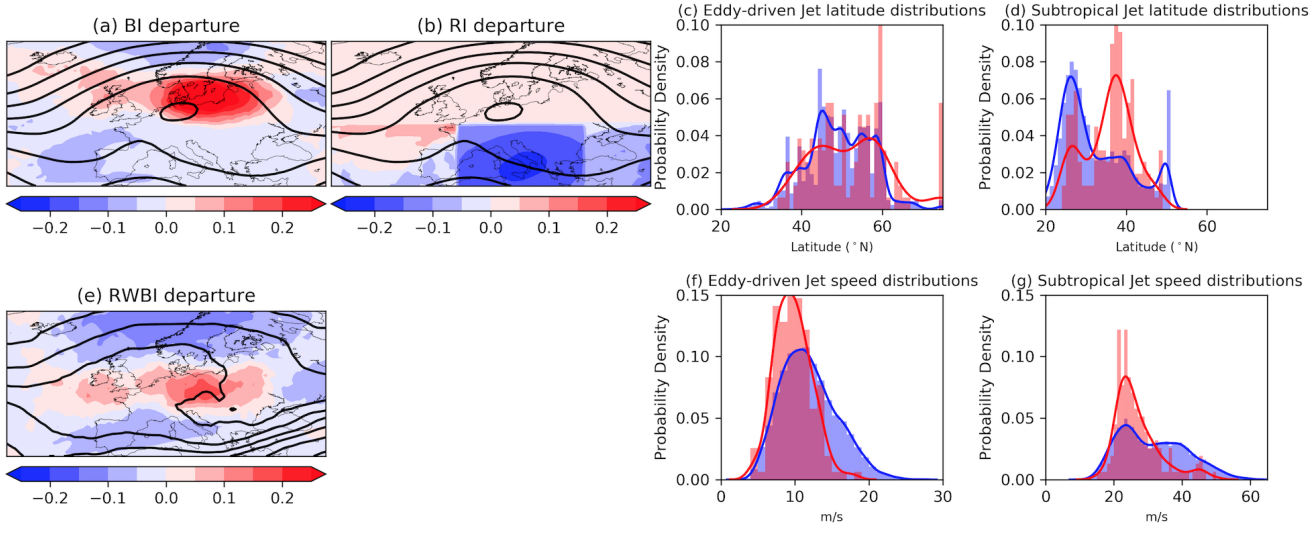

Figure 3. As in Figure 2 but for stagnation in NEU.

In Figure 3, composites of the large-scale circulation for stagnation in NEU are shown as a representation of northern Europe (SCAN, NEU and CEU). Stagnation occurring in northern regions is associated with a large increase in block frequency over the stagnant area, seen also as an amplified large-scale wave in Z500 (Fig. 3(a), (b)). For NEU, it extends from the UK across most of Europe and a cut off region of high pressure is evident at its centre with the increase in block frequency exceeding 25%. The flow reversal associated with this blocking pattern also involves lower pressures and hence a strong reduction in subtropical ridge frequency south of the block structure (Fig. 3 (b)). The large-scale, upper-level wave is also seen in the mean potential temperature field on the dynamical tropopause, which features an anticyclonically breaking Rossby wave. This corresponds to an increase of anticyclonic RWB slightly south of the region of increased block frequency. The eddy-driven jet is less frequently in its central mode (Fig. 3 (c)) as it would typically result in strong winds not conducive to stagnation over

https://doi.org/10.5194/wcd-2021-5
Preprint. Discussion started: 27 January 2021

the regions, and shows the largest departures in northern latitudes (poleward of 60°N). Differently, the subtropical jet latitude exhibits a strong increase in the central latitudes of its distribution (around 40°N), reflecting the southern branch of the split jet pattern associated with the block. Both jet streams are also significantly less intense during NEU stagnation ($p<0.01$): the distributions of jet speed are both notably shifted toward lower wind speeds (Fig. 3 (f), (g)). Blocking and RWB are also more frequent for stagnation in SCAN and CEU and are also associated with amplified upper-level waves centred over the regions (not shown). The reduction in ridge frequency during stagnation in NEU is present for SCAN but not for stagnation in the more equatorward latitudes of CEU. For stagnation in CEU and SCAN, the eddy-driven jet is less frequently over the latitudinal ranges encompassed by these regions (the southern and northern modes, respectively), and the subtropical jet index captures the southern branch of the blocking-induced split jet pattern in both regions.

Summing up, the dynamical signatures of stagnation as inferred from the composited departures of the dynamical indices are larger for northern regions in Europe. The comparatively weaker anomalies for the southern regions reflect the fact that the mean weather conditions in southern Europe are more favourable (drier and less windy) for stagnation. This does not however mean that stagnation in southern regions is less related to the large-scale circulation. Finally, the composites shown in Figures 2 and 3 are for stagnation defined by the Horton et al. (2012) index. Repeating the analysis using the Wang et al. (2018) and Huang et al. (2018) indices gives very similar results (not shown) and suggests that the large-scale circulation signatures highlighted are indeed important for stagnant air occurrence and not a feature of the chosen ASI. The composites of the large-scale flow are also similar when considering stagnation in each season separately (not shown), suggesting that stagnation occurs under similar set ups of the large-scale flow in all seasons. The seasonality of the large-scale connection to stagnation is further explored in the remainder of this section.

3.2 Seasonal and lag dependence of the large-scale circulation

Stagnation events occurring year-round have been examined so far. Now we explore the seasonality and time dependence of the relationship between the large-scale dynamics and air stagnation. To do this, we define a metric quantifying the correspondence between stagnation and selected dynamical indices. We term this the *departure measure* and define it as

$$\frac{1}{N_R}\sum_{i\in R}|I_{stagnation} - I_{climatology}|, \tag{2}$$

where R is the region, i a grid point within region R, N_R is the number of grid points in the region and I is the dynamical index. For simplicity, this subsection excludes large-scale dynamical factors (i.e. jet streams) and focuses on the most immediate regional drivers (block, RWB and ridge index-frequency), for which lagged relationships can be better interpreted. The departure measure is thus unitless. The Rossby wave breaking index is included for all regions while the block and ridge indices are shown only for regions where they are most influential (northern and southern regions, respectively; Section 3). In addition, the four day persistence criteria is removed here to ensure enough stagnant days are included in the analysis, which is necessary when considering northern regions in winter.

Departure measures as a function of lag about stagnant day are shown in Figure 4, for each region, season and dynamical index. There are three features to highlight in Figure 4. Firstly, the large-scale dynamics and stagnation correspondence tends

https://doi.org/10.5194/wcd-2021-5
Preprint. Discussion started: 27 January 2021

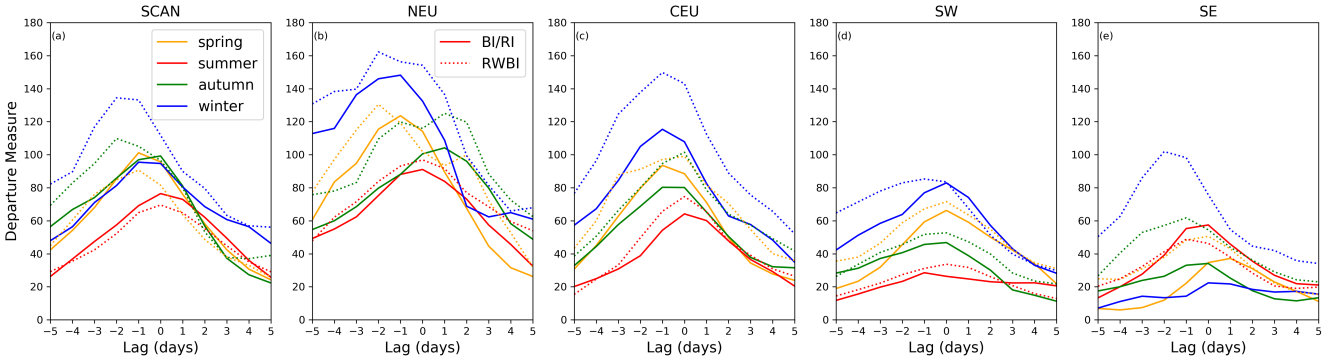

Figure 4. Departure measures for the blocking or ridge index (solid lines), and the Rossby wave breaking index (dotted lines) during stagnation for each season as a function of lag from stagnant days in (a) SCAN, (b) NEU, (c) CEU, (d) SW and (e) SE. The blocking index is shown for SCAN, NEU and CEU and the ridge index for SW and SE.

to be strongest in winter (departure measure is largest), except for ridges in SE which peak in summer (Fig. 4 (e)) and blocks in SCAN which peak in spring (although with departure measures very close to those in autumn and winter, Fig. 4 (a)). Air stagnation is more closely related to the large-scale circulation in winter because calm, dry conditions are rarer at this time of year, and need to be driven by a synoptic-scale anticyclone more frequently. Secondly, the departure measures for SCAN, NEU and CEU are higher than in SW and SE, involving larger departures of the atmospheric circulation. This again relates to the less favourable weather conditions for stagnation in northern regions, which means that larger anomalies are required therein for stagnation to occur, as compared to southern regions. Finally, the large-scale dynamics leads the changes in air stagnation by a few days. This can be inferred from the peak in departure measure for negative lags. This lag between the large-scale dynamics and air stagnation could have implications for the predictability of air stagnation.

Concerning the specific regional drivers, overall, stagnation is around 30% more likely to occur when there is a block or ridge present, though this number is sensitive to the precise definition of a region being blocked or ridged (not shown). The increase in stagnation for a given driver also depends on the region and season. A ridge being present in SW and SE increases the occurrence of stagnation in those regions considerably (on average, around 75% of ridge days are also diagnosed as stagnant), particularly in summer. On days identified as having a block in SCAN, NEU and CEU the frequency of stagnation is increased on average by more than 40% for all seasons. Rossby wave breaking also increases the likelihood of stagnation occurring in SCAN and NEU (by around 25%) but has no clear impact for the southern regions. We now explore to what extent the large-scale circulation can explain the variability in air stagnation.

4 Modelling the variability of European air stagnation

In this section, the MLR method described in section 2.3 is used to model the monthly variability of air stagnation. The monthly count of stagnant days in each region and season is modelled separately using the dynamical indices as predictors. A day is

https://doi.org/10.5194/wcd-2021-5
Preprint. Discussion started: 27 January 2021

Weather and Climate Dynamics Discussions
Open Access
EGU

counted as stagnant if the number of stagnant grid points in the region is above its 50th percentile in the climatology. The results presented in this section are robust to the choice of this threshold. The dynamical indices are used as predictors as follows. The blocking (BI), Rossby wave breaking (RWBI), and ridge (RI) indices are regionalized as the number of days in a month when the region was dominated by such weather systems, which occurs if the number of affected grid points is above its 50th percentile. As mentioned above, ridges are only considered for CEU, SW and SE. The monthly mean latitude and speed of the eddy-driven (JL and JS) and subtropical (STJL and STJS) jets are used as direct predictors (the time series of these predictors are the same for every region). Recall that we only use regional or large-scale predictors (based on $Z500$, wind speed throughout the troposphere, and θ on 2 PVU) to quantify the percent of variance in stagnation that can be explained from the dynamics, without including smaller-scale or local phenomena, such as local winds or convection. We exploit the stepwise procedure to identify the large-scale dynamical processes most related to air stagnation as follows.

The stepwise MLR models are constructed for each region and season. All regions share the jet-based predictors, as they are defined independently of the region (i.e. Europe-wide). For the remaining drivers (BI, RWBI, RI), each region has its own set and time series of predictors that account for regional information on the frequency of occurrence of synoptic-scale systems, with RI being included only for those regions where ridges occur (SW, SE and CEU). For example, we model the monthly variability of air stagnation in SCAN (AS_{SCAN}) as

$$\mathrm{AS}_{SCAN} \approx \beta_0 + \beta_1 \mathrm{BI}_{SCAN} + \beta_2 \mathrm{RWBI}_{SCAN} + \beta_3 \mathrm{JL} + \beta_4 \mathrm{JS} + \beta_6 \mathrm{STJL} + \beta_6 \mathrm{STJS}, \tag{3}$$

where BI_{SCAN} and RWBI_{SCAN} are the monthly time series of blocked days in SCAN and RWB days in SCAN respectively. β_0 is the model intercept and the β_i terms are the regression coefficients.

In addition, for each region we construct a second model that also incorporates the regional predictors defined for the remaining regions. By including the time series of BI, RWBI and RI for all regions we can account for remote influences of the atmospheric circulation on air stagnation. These synoptic systems can have a remote (non-local) impact on stagnation by influencing the weather conditions both upstream and downstream of their location. Therefore, the second model expands the set of predictors by considering those that are specific of the other regions. Using stagnation in SCAN as an example again, this second model is constructed as

$$\mathrm{AS}_{SCAN} \approx \sum_{regions} \mathrm{BI}_R + \sum_{regions} \mathrm{RWBI}_R + \sum_{regions} RI_R + \mathrm{JL} + \mathrm{JS} + \mathrm{STJL} + \mathrm{STJS}, \tag{4}$$

where subscript R refers to the region of the index time series included. As in equation 3, the model includes an intercept and regression coefficients but they are omitted here for clarity. For both models, the stepwise procedure is subsequently applied to select the leading predictors and avoid the inclusion of predictors that are too highly correlated with one another. We term the first model (equation 3) the regional model and the second (equation 4) the European model for the remainder of this section.

4.1 Variance in stagnation explained by the dynamical predictors

The coefficients of determination (R^2) for the regional and European stepwise MLR models are presented in Figure 5. Between 30 and 50% of the monthly variability of air stagnation can be explained by the regional models in most cases, though this

https://doi.org/10.5194/wcd-2021-5
Preprint. Discussion started: 27 January 2021

is dependent on region and season. For instance, more than 50% of the variance in stagnation in NEU can be explained by the regional model for most seasons, whereas it is less than 25% for SCAN in spring. This increases to between 40 and 70% when including remote predictors in the regression, highlighting the faraway effect weather systems, such as blocks and ridges, can have on the surface weather. Both model set ups give a statistically significant relationship between air stagnation and the large-scale circulation for all regions and seasons ($p<0.01$). The model skill is generally highest in winter, consistent with the closer association between stagnation and the large-scale circulation in winter shown in section 3. The model does not perform better in northern or southern regions in Europe: model skill is similar in SW, CEU and NEU and generally lowest in SCAN and SE. This suggests that weaker circulation anomalies can have a comparatively larger effect in southern compared to northern regions, such that smaller departure measures (Fig. 4) in southern regions can lead to R^2 values as high as those in northern regions.

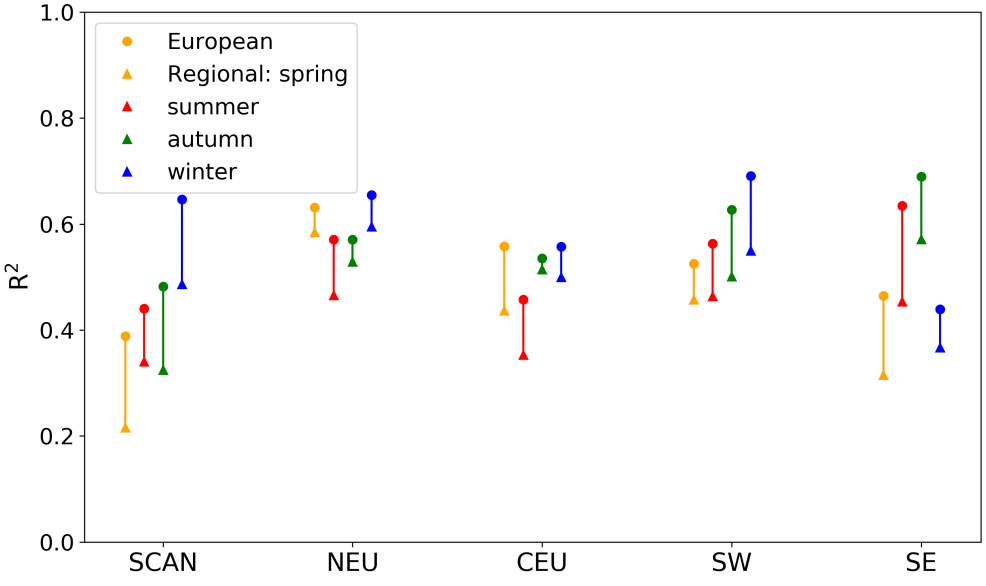

Figure 5. Skill of the stepwise multiple linear regression models (R^2) of air stagnation in each region and season (colours). Skills are shown for the regional models (triangles) and the European models (circle). See text for an explanation of the regional and European models.

Comparing the explained variance between the two models gives insight into which seasons and regions are most affected by the remote drivers. Overall, the remote predictors compensate for the lower skill of local predictors in SCAN and SE in most seasons (R^2 increases greater than 0.15). They add comparatively lower skill in NEU and CEU in the cold seasons and SW in the warm seasons. The variance in stagnation explained by the European models in these regions is more consistent across seasons than that obtained from the regional models. As regional predictors are favourable for stagnation in the region they occur, we hypothesize that the remote predictors most likely bring model improvements by informing the occasions when stagnation is disfavoured in the region, i.e. they have a negative coefficient in the MLR equation.

https://doi.org/10.5194/wcd-2021-5
Preprint. Discussion started: 27 January 2021

Weather and Climate Dynamics Discussions
Open Access
EGU

4.2 Dynamical predictors of air stagnation

The predictors selected by the stepwise regression method are discussed in this section for each region and season. We now only consider the European model that uses both local and remote predictors as it consistently outperforms the regional model. The predictors selected by the model represent the dynamical drivers that are needed to explain the most variance in air stagnation. There are a total of 17 predictors for the stepwise method to select from: five regional BI and RWBI predictors (one for each region), three RI predictors (for CEU, SW and SE), together with the jet latitude and speed time series for the eddy-driven and subtropical jets. The model skill (R^2) achieved by the selected predictors are shown for each season and region in Figure 6. The model skills shown in the maps correspond to the R^2 values reached after adding the final predictor into the model.

First we detail some statistics about the selected large-scale predictors for air stagnation. The number of predictors necessary to include in the MLR model of air stagnation varies between 4 and 12, depending on the region and season. The average number of predictors included in the model is about 7 for SCAN and NEU and 9 for CEU, SW and SE. Therefore, fewer predictors are typically required to explain stagnation variability in northern regions. The colours behind each included predictor show the model R^2 as each of the predictors is added (from left to right) in the formulation. In some cases, one predictor can explain a large fraction of the variance, for example in NEU winter stagnation, and the additional predictors add relatively little skill to the model (though still more than the 1% threshold required by the stepwise formulation). Other times, more predictors have a more equal contribution to the overall model skill, for example when describing stagnation in SW winter. This does not necessarily impact the overall skill of the model, which is in both cases above 60% of monthly stagnation variability.

The leading predictors for regional air stagnation are most often RWB and blocking (each 7 times out of the total 20 region/season combinations), with ridges and the subtropical jet speed being the leading predictor in 3 combinations each. Many regions and seasons include both RWBI and BI as predictors (in a few cases from the same regions). Despite their apparent similarity, these two indices can reflect different block configurations and persistent signatures, as stated above, which may partly explain this result. Out of the 20 leading predictors 12 have a positive contribution to the model (8 have negative) and 9 are local processes (11 remote drivers), although these figures are all dependent on the region and the season considered. We recall that in many cases the difference in explained variance between a given predictor and the following one is small. Therefore, the specific order in which predictors are selected may not be necessarily meaningful from a dynamical point of view.

In spite of these limitations, we can use the stepwise regression results to make some inferences on the dynamical influences. In SCAN, RWB and blocking occurring locally dominate stagnation variability. Only in winter are both predictors included by the model, though, suggesting the indices are identifying different features in this season. BI and RWBI occurring in other regions (south of SCAN) inform stagnation reduction (negative coefficient), because they are associated with a poleward strengthening of zonal winds and hence increased wind speeds over SCAN. Subtropical ridges in SE and CEU have similar effects (e.g. Sousa et al., 2018), in agreement with their negative contribution to stagnation frequency. The eddy-driven jet is not identified as an important driver for stagnation in SCAN (only appearing twice as the final predictor selected in the model) supporting the results of Madonna et al. (2017) who found that variations in Scandinavia blocking and the eddy-driven jet are

https://doi.org/10.5194/wcd-2021-5
Preprint. Discussion started: 27 January 2021

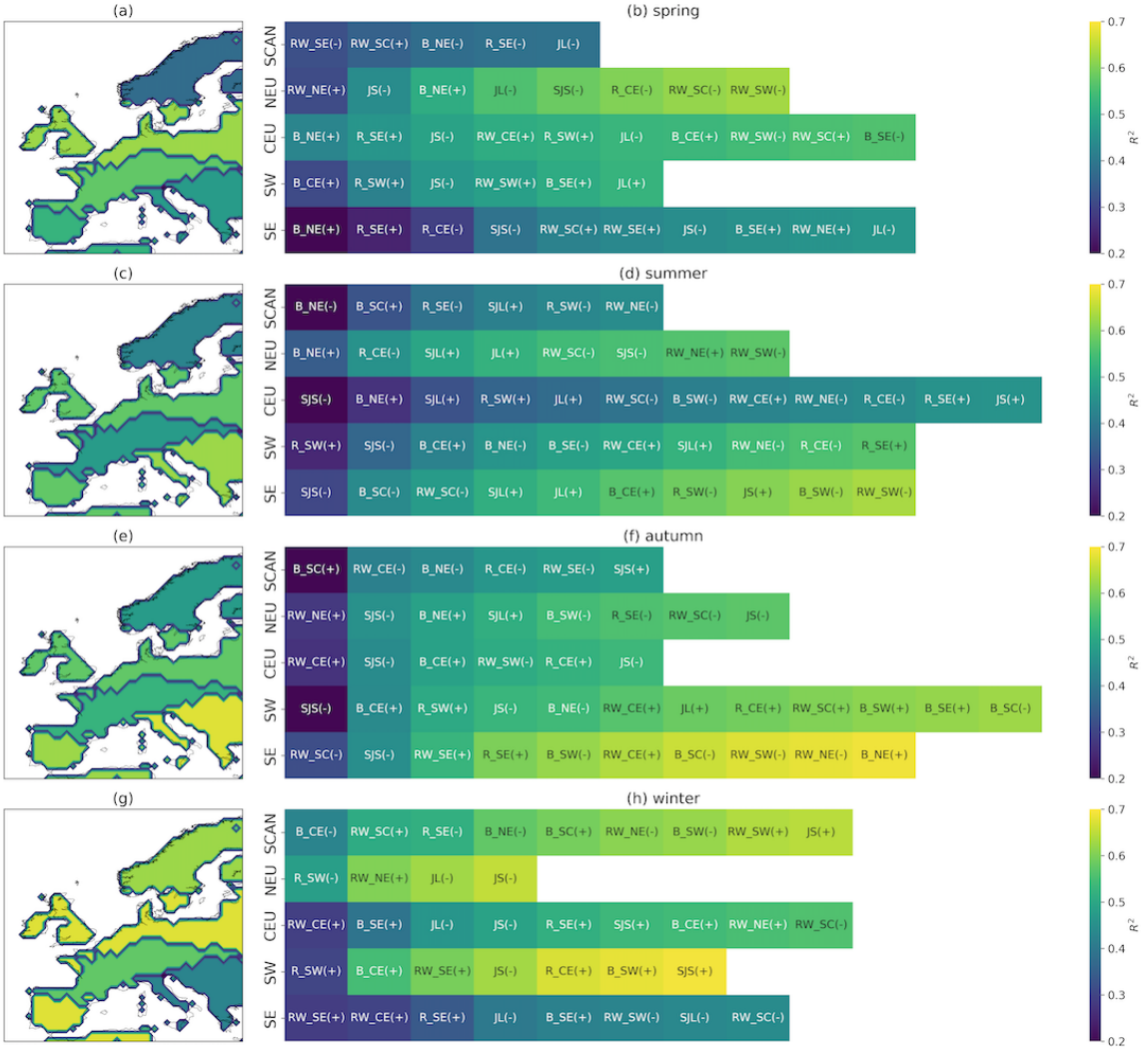

Figure 6. Model R^2 for stagnation occurring in (a) spring, (c) summer, (e) autumn and (g) winter. Predictors included in the stepwise linear regression for each region in (b) spring, (d) summer, (f) autumn and (h) winter, where the plus and minus signs for each predictor represent whether the coefficient in the MLR model is positive or negative, respectively. Colours in the right hand panels show the R^2 of the model as each predictor is added in its formulation. The R^2 values are calculated for monthly data in 1979–2018.

relatively unconnected. The poleward strengthening of the zonal wind associated with blocks and ridges occurs outside the region of the eddy-driven jet index. The subtropical jet is also not important for stagnation in SCAN, which is expected as this region is too far north.

Local blocking or RWB also drive stagnation in NEU, appearing as the leading predictor in every season except winter (when it appears second). Winter stagnation in NEU is neatly described using only four predictors. It is favoured by local RWB

https://doi.org/10.5194/wcd-2021-5
Preprint. Discussion started: 27 January 2021

and reduced when the eddy-driven jet is strong and located over this region, as inferred from the negative terms for JS and JL, as well RI over SW. On the other hand, subtropical ridges reduce stagnation in NEU in the other seasons by shifting the jet stream over the region. Indeed, the eddy-driven jet is an important predictor for NEU across all seasons, as this region lies at the jet exit region and will be more directly impacted by its characteristics.

In CEU, both local and remote occurrences of blocking and RWB influence stagnation occurrence. This region covers a relatively small region meridionally, smaller than the typical meridional scale for a blocking event, so a block situated over NEU or SE would also be expected to extend over CEU and favour stagnation therein. Blocking and RWB in CEU, NEU and SE are thus typically positive predictors in the model, with the exception of Rossby wave breaking over NEU in summer when it only appears as the ninth predictor. RWB in SCAN can have a positive or negative influence on stagnation in CEU, depending on the season (although the amount of variance explained by this predictor is often small). This behaviour could reflect seasonal changes in the latitude of RWB or in the associated pattern. For example, a dipole-type block over SCAN would be associated with a cyclonic circulation anomaly over CEU and hence increased wind, and a reduction in stagnation likelihood. An omega-type block may extend across parts of both SCAN and CEU and bring settled anticyclonic conditions to both regions. Stagnation in CEU is typically reduced when the eddy-driven jet speed is increased. The opposite is true in summer, when the eddy-driven jet shifts north towards latitudes farther from CEU. Local ridges are not as important for stagnation in CEU, appearing further down the list of predictors, arguably because they involve large meridional excursions form their subtropical sources and tend to break, therefore being better described by the RWBI or BI.

In contrast to CEU, subtropical ridges are key for stagnation variability in SW, appearing twice as the leading predictor and once as the second included predictor. They bring sunny, settled conditions over SW and can thus support stagnation occurrence (e.g. Santos et al., 2009). The so-called low-latitude blocking events (i.e. those occurring in SW and SE) can be easily confounded with subtropical ridges (Sousa et al., 2018), which sometimes expand over vast subtropical regions and hence can also promote stagnation in SW. Blocking systems centered polewards of SW, such as those in CEU, can also extend over their anticyclonic influence over SW depending on their location, scale and shape. The subtropical jet speed is a key predictor for SW stagnation in summer and autumn when a weaker subtropical jet favours stagnation occurrence. In winter, the subtropical jet is situated further south than the SW region so it will not directly impact stagnation therein (it appears as the last predictor, with positive sign and adds a small amount of explained variance). Increases in the eddy-driven jet speed also predict a reduction in SW stagnation for all seasons except summer, when the eddy driven jet is located at its northernmost latitudes.

Although local blocking and RWB also tend to dominate stagnation variability in SE, the dynamical predictors are more numerous and seasonally-varying in this region than in the others. A strong subtropical jet reduces stagnation in all seasons but winter. Highlighting a similar same weather pattern, local ridges are associated with increased stagnation in most seasons. In spring, when blocking reaches large areal extents, the leading predictor of SE stagnation is blocking in the neighbouring region of NEU. As the SE region is farther downstream of the North Atlantic, the eddy-driven jet speed and latitude are not identified as important drivers of regional stagnation.

Thus far, we have given a broad explanation of some of the key predictors of stagnation in each region. A complete explanation of the predictors related to stagnation in every region and season is unfeasible, so, as an example, air stagnation occurring

https://doi.org/10.5194/wcd-2021-5
Preprint. Discussion started: 27 January 2021

in SW during winter is explored further, which is the combination yielding the highest skill. The leading five predictors are included in our discussion. They are local subtropical ridges, blocking in CEU, RWB over SE, the eddy driven jet speed, and subtropical ridges over CEU. To aid in the explanation two measures are considered. Firstly, the partial correlation in the MLR model between the stagnation time series and each predictor is calculated. The partial correlations are similar for each of these predictors and so none of the large-scale features dominate over the others. Secondly, composites of air stagnation frequency anomaly are produced for the four selected predictors that are defined regionally. The composites are produced by comparing stagnation occurring on days when each predictor index covers half the region to the climatological frequency of stagnation (the same method for the composites shown in Section 3). Whilst these composites do not reflect the linear behaviour of the MLR model, they do demonstrate the direct impact the predictors have individually on the occurrence of air stagnation and are useful when interpreting the stepwise model results.

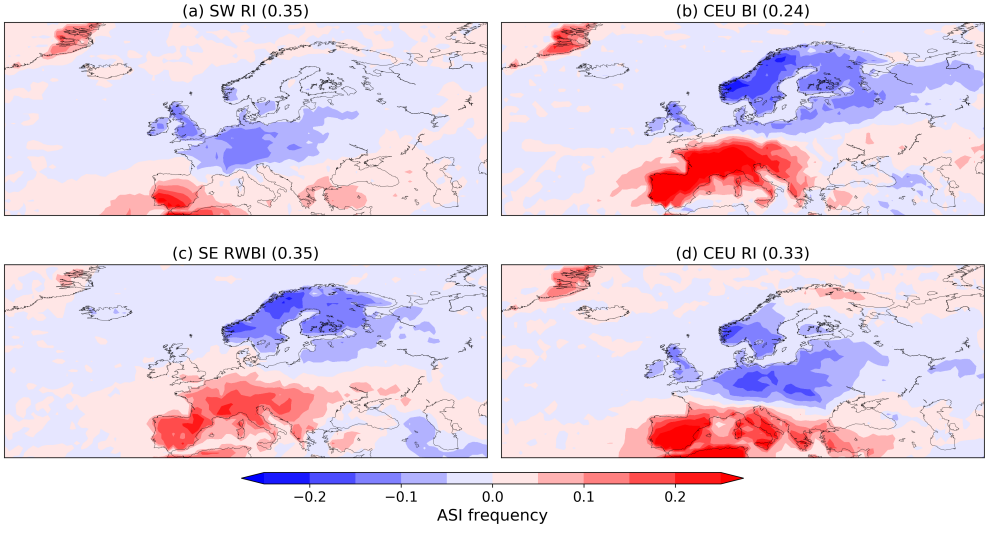

Figure 7. Composite departures (colour shading) and partial correlations (numbers in brackets on top of panels, based on monthly data) of stagnation occurrence in winter for days with (a) subtropical ridges in SW, (b) blocking in CEU, (c) Rossby wave breaking in SE and (d) subtropical ridges in CEU. These are among the five leading terms in the stepwise model for stagnation in SW winter.

Subtropical ridges identified in SW and the contiguous CEU region are both associated with increased stagnation frequencies in SW. The associated anomalously high geopotential height in these regions promotes anticyclonic circulation and settled conditions with suppressed rainfall, which favour stagnation. The influence of SW ridges is locally restricted whereas ridges in CEU promote stagnation across the Mediterranean (Fig. 7 (a), (d)). SW ridges are likely related to those defined as Atlantic ridges in Sousa et al. (2018) and hence are associated with stronger winds north of SW, where stagnation is reduced. Ridges identified in CEU will also include European ridges in the definition of Sousa et al. (2018) associated with high geopotential heights across the region. Blocking in CEU has a similar effect (Fig. 7 (b)). Blocks in this region often develop from subtropical

https://doi.org/10.5194/wcd-2021-5
Preprint. Discussion started: 27 January 2021

ridges extending from lower latitudes and are identified by the block index when the ridge begins to overturn. This typically begins anticyclonically on the eastern flank of the ridges and hence block onsets in this region are typically identified as anticyclonic (Masato et al., 2012). This means that the area to the south and east of the block remains in a region of anticyclonic circulation with conditions favourable for stagnation as the ridge develops. This feature is evident in the composite of block frequency for SW stagnation (Fig. 2 (a)) as an increase in block frequency extending from SW into CEU with a SW-NE orientation. The fourth predictor has a negative regression coefficient and describes the eddy-driven jet speed. Strong winds are obviously not conducive for stagnation occurrence, particularly when the jet is located in its southern mode which is directly above SW (Fig. 2 (c)). SW stagnation is also more frequent on days defined as having Rossby wave breaking in SE. Anticyclonic RWB can occur over SE as a result of the regional meridional shear of the zonal wind (i.e. when mid tropospheric winds intensify to the north of the region and/or weaken over SE). This is expected to enhance the SE-NE tilt of the eddy-driven jet, diverting cyclone tracks away from southern Europe and the Mediterranean. On the other hand, RWB in SE can also be a regional signature of anticyclonic RWB on the eastern flank of a large-scale European block extending its anticyclonic influence (weak winds and absence of precipitation) towards SW. The large-scale circulation pattern would resemble that in Figure 3 (e), but shifted to the south.

4.3 Comparison with other ASIs

All of the results included in the article thus far have been obtained using the ASI of Horton et al. (2012). In this section the European stepwise MLR is repeated for modelling the monthly variability of air stagnation in the Huang et al. (2018) and Wang et al. (2018) ASIs. The Horton et al. (2012) ASI includes the wind speed at 500 hPa in its formulation whereas the Huang et al. (2018) and Wang et al. (2018) ASIs contain no criteria based on the flow at upper levels.

The skill of the models of each ASI variability are shown in Figure 8, for each region and season. Generally, the skill of the model is quite consistent across the ASIs, although the model does slightly better for the Horton et al. (2012) index in most seasons and regions. The overall consistency implies that the ASI does not need a criterion based on the mid-tropospheric flow for the large-scale dynamics to be able to explain a significant amount of the variability. The largest difference in skill is seen for stagnation in the SW summer (Fig. 8 (d)). This reflects the fact that the upper-level wind is the controlling variable defining stagnation in the Horton et al. (2012) index in SW summer. Indeed, removing the upper-level wind criterion from the Horton et al. (2012) index in SW summer reduces the amount of variance that can be explained by the dynamics (R^2 reduces from 0.563 to 0.496, not shown). This loss of explained variance also implies that the large-scale dynamics may be less related to precipitation in SW summer, since precipitation is the common variable in the three ASIs. In fact, precipitation in SW summer is infrequent and typically associated with mesoscale features. The small difference in skill between models of the three ASIs for the other regions and seasons shows that the results are robust and that the large-scale circulation is important for regional air stagnation in Europe.

https://doi.org/10.5194/wcd-2021-5
Preprint. Discussion started: 27 January 2021

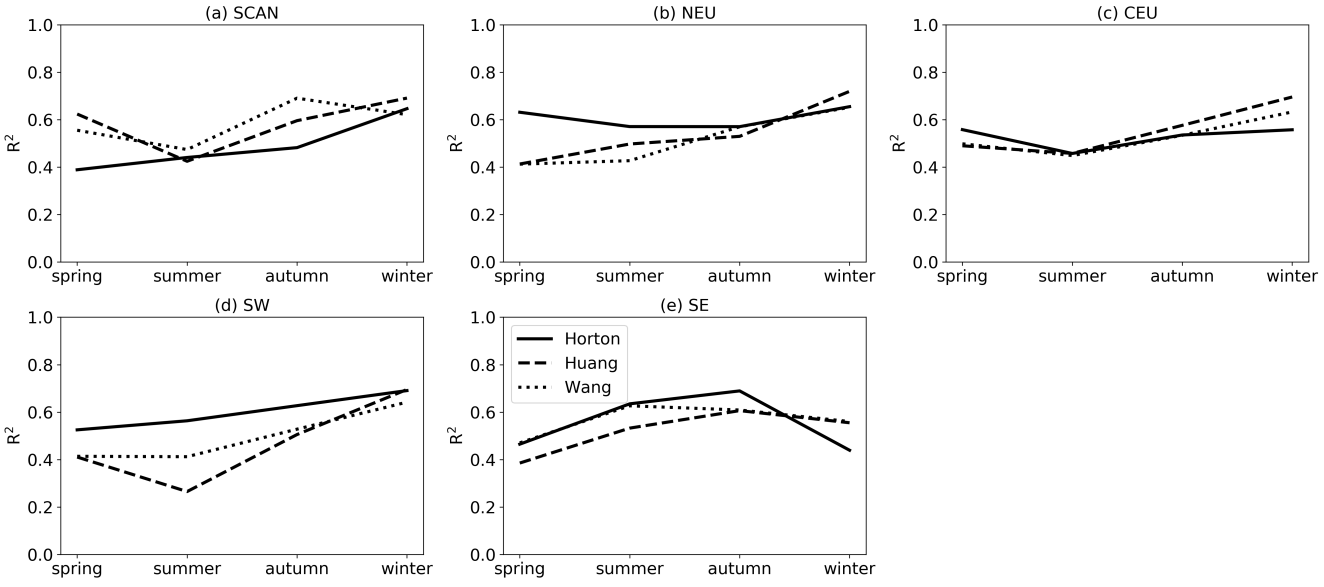

Figure 8. Stepwise multiple linear model skill for air stagnation in (a) SCAN, (b) NEU, (c) CEU, (d) SW and (e) SE defined using the Horton (solid), Huang (dashed) and Wang (dotted) indices.

5 Conclusions

Air stagnation is known to have a large influence on air quality (e.g. Jacob and Winner, 2009; Garrido-Perez et al., 2018; Toro et al., 2019). As poor air quality is hazardous to human health (Pope III et al., 2002; Cohen et al., 2017), it is crucial to understand the processes causing air stagnation. Different local meteorological conditions have been shown to drive both air stagnation events and the build-up of specific pollutants in particular regions and seasons (Prtenjak et al., 2009; Dawson et al., 2014; Zhang et al., 2014). However, the large-scale circulation features driving such local conditions have comparatively been poorly addressed and are here used to describe air stagnation characteristics within Europe.

In the present paper, air stagnation in Europe is shown to be strongly influenced by the large-scale circulation. Moreover, the large-scale leads changes in stagnation by a few days, which could have implications for its predictability. The large-scale circulation more often resembles a synoptic-scale high pressure system when stagnation is present. For northern regions this is achieved through the presence of an atmospheric blocking event whereas in southern regions it is more typically associated with subtropical ridges. Indeed, subtropical ridges are unfavourable for stagnation in northern Europe, as they are associated with a poleward strengthening of winds which is unfavourable for stagnation. Similarly, stagnation in Southern Europe is less frequent during high latitude blocking events (when strong winds and low pressure systems are diverted to the south of the block). These results are generally consistent with previous studies linking air stagnation or pollutant build up with large-scale meteorological drivers such as blocking and subtropical ridges (Garrido-Perez et al., 2017; Ordoñez et al., 2017), the position of the midlatitude jets (Barnes and Fiore, 2013; Shen et al., 2015; Ordóñez et al., 2019; Kerr et al., 2020a,b), Rossby wave

https://doi.org/10.5194/wcd-2021-5
Preprint. Discussion started: 27 January 2021

breaking (Webber et al., 2017), or cyclone frequency (Leibensperger et al., 2008; Tai et al., 2010, 2012; Leung et al., 2018), but our results provide a complete picture for stagnation events occurring year-round across Europe and allow discerning the relative roles of these multiple drivers.

Multiple linear regression models using a stepwise selection procedure have been used to model the monthly variability of regional air stagnation in each region and season. Dynamical indices describing the large-scale circulation can be used to model the monthly variability of air stagnation and can explain around 60% of its variance. The model generally performs best when predicting stagnation in winter, particularly in SCAN. Winter weather conditions are typically windier and wetter than in other seasons so for stagnation to occur it is more likely to be driven by a large-scale circulation feature. This means stagnation and the large-scale flow are more closely related and the model skill is higher. Furthermore, surface weather conditions are more strongly controlled by circulation changes in winter than in summer (Vautard and Yiou, 2009). The amount of variance explained by the large-scale circulation increases when including both local and remote predictors in the statistical model, particularly in cases when local phenomena are able to explain relatively little of the stagnation variability. Synoptic scale weather systems influence weather in upstream and downstream regions and are able to affect stagnation both locally and remotely.

The conclusions drawn from the results presented in this paper are robust to the choice of air stagnation index. The large-scale circulation shows similar signatures for the air stagnation events defined by three different indices, and is able to explain a similar amount of their variability, though for some regions and seasons the large-scale circulation shows stronger influences on the Horton et al. (2014) index, which also accounts for upper-level winds. Each of the stagnation indices considered here have been shown to identify situations in which pollutants can build up in various regions of the globe (Schnell and Prather, 2017; Garrido-Perez et al., 2018; Liao et al., 2018; Huang et al., 2018; Garrido-Perez et al., 2021), though air stagnation and pollution are not always strongly connected (Kerr and Waugh, 2018; Garrido-Perez et al., 2019). Indeed, the high variability of air stagnation explained by the large-scale circulation is similar to the variability of ozone and PM explained by meteorological parameters (Ordóñez et al., 2005; Barmpadimos et al., 2011, 2012; Carro-Calvo et al., 2017). This suggests that the variance in air stagnation explained by the large-scale circulation can be used to understand pollutant variability, as well as changes in future high pollution episodes, which is what is most important to understand for health related climate impacts.

Air stagnation is generally expected to become more frequent with climate change (Leung and Gustafson Jr, 2005; Horton et al., 2012, 2014; Caserini et al., 2017). Projected increases in temperature, reductions in precipitation and cyclone frequency, and shifted jet streams contribute to the projected increase in stagnation (Mickley et al., 2004; Leung and Gustafson Jr, 2005; Horton et al., 2012, 2014; Caserini et al., 2017), which can result in increased pollutant levels (Weaver et al., 2009; Jacob and Winner, 2009). In addition, air stagnation and high pollution episodes tend to coincide with heatwaves during summer (Schnell and Prather, 2017), exacerbating the health impacts of each phenomenon, so understanding and trusting future changes in them is crucially important. In Horton et al. (2014), a bias correction was needed to account for climate model deficiency in simulating conditions favourable for air stagnation. Caution must be taken when analysing bias-corrected climate model output, as it cannot overcome all model errors or correct model variability (Maraun et al., 2017), and can alter relationships between variables and break conservation principles (Ehret et al., 2012). The identification of air stagnation in climate models uses

https://doi.org/10.5194/wcd-2021-5
Preprint. Discussion started: 27 January 2021

meteorological variables that climate models may struggle to represent, such as precipitation and near-surface wind speeds (Flato et al., 2013). Climate model simulations are expected to better represent features of the large-scale circulation than the variables used to compute air stagnation indices. Therefore, the findings presented in this paper can be used to evaluate the reliability of air stagnation in climate models and assess their future changes. The large-scale circulation and stagnation correspondence in climate model simulations will be presented in a future article.

Data availability. The ERA5 reanalysis used in this study is available from the European Center for Medium-range Weather Forecasts website (https://www.ecmwf.int/en/forecasts/datasets/reanalysis-datasets/era5).

Author contributions. JMGP calculated the air stagnation indices as defined in Wang et al. (2016, 2018) and Huang et al. (2017). JM performed the rest of the analyses in this study and wrote the manuscript. MA, DB, RGH and CO contributed to the interpretation of the results and the writing of the paper.

Competing interests. The authors declare that they have no conflict of interest.

Acknowledgements. This work has been funded by the Spanish Ministerio de Economía, Industria y Competitividad under grant CGL2017-83198-R (STEADY) and Ministerio de Ciencia Innovación y Universidades, under grant RTI2018-096402-B-I00 (JeDiS). MA was supported by the Program Atracción de Talento de la Comunidad de Madrid (2016-T2/AMB-1405), JMGP by a predoctoral research grant awarded by the Spanish Ministerio de Educación, Cultura y Deporte (FPU16/01972) and CO by the Ramón y Cajal Programme of the Spanish Ministerio de Economía y Competitividad (RYC-2014-15036).

https://doi.org/10.5194/wcd-2021-5
Preprint. Discussion started: 27 January 2021

Weather and Climate Dynamics Discussions
Open Access
EGU

References

Barmpadimos, I., Hueglin, C., Keller, J., Henne, S., and Prévôt, A.: Influence of meteorology on PM_{10} trends and variability in Switzerland from 1991 to 2008, Atmospheric Chemistry and Physics, 11, 1813, 2011.

Barmpadimos, I., Keller, J., Oderbolz, D., Hueglin, C., and Prévôt, A.: One decade of parallel fine ($PM_{2.5}$) and coarse (PM_{10}–$PM_{2.5}$) particulate matter measurements in Europe: trends and variability, Atmospheric Chemistry and Physics, 12, 3189–3203, 2012.

Barnes, E. A. and Fiore, A. M.: Surface ozone variability and the jet position: Implications for projecting future air quality, Geophysical Research Letters, 40, 2839–2844, 2013.

Barriopedro, D., García-Herrera, R., and Trigo, R. M.: Application of blocking diagnosis methods to general circulation models. Part I: A novel detection scheme, Climate dynamics, 35, 1373–1391, 2010.

Carro-Calvo, L., Ordóñez, C., García-Herrera, R., and Schnell, J. L.: Spatial clustering and meteorological drivers of summer ozone in Europe, Atmospheric Environment, 167, 496–510, 2017.

Caserini, S., Giani, P., Cacciamani, C., Ozgen, S., and Lonati, G.: Influence of climate change on the frequency of daytime temperature inversions and stagnation events in the Po Valley: historical trend and future projections, Atmospheric Research, 184, 15–23, 2017.

Cohen, A. J., Brauer, M., Burnett, R., Anderson, H. R., Frostad, J., Estep, K., Balakrishnan, K., Brunekreef, B., Dandona, L., Dandona, R., et al.: Estimates and 25-year trends of the global burden of disease attributable to ambient air pollution: an analysis of data from the Global Burden of Diseases Study 2015, The Lancet, 389, 1907–1918, 2017.

Comrie, A. C. and Yarnal, B.: Relationships between synoptic-scale atmospheric circulation and ozone concentrations in metropolitan Pittsburgh, Pennsylvania, Atmospheric Environment. Part B. Urban Atmosphere, 26, 301–312, 1992.

Dawson, J. P., Bloomer, B. J., Winner, D. A., and Weaver, C. P.: Understanding the meteorological drivers of US particulate matter concentrations in a changing climate, Bulletin of the American Meteorological Society, 95, 521–532, 2014.

Ehret, U., Zehe, E., Wulfmeyer, V., Warrach-Sagi, K., and Liebert, J.: Should we apply bias correction to global and regional climate model data?, Hydrology & Earth System Sciences, 9, 3391–3404, 2012.

European Environment Agency: Air quality in Europe — 2020 report, https://www.eea.europa.eu//publications/air-quality-in-europe-2020-report, 2020.

Flato, G., Marotzke, J., Abiodun, B., Braconnot, P., Chou, S., Collins, W., Cox, P., Driouech, F., S. Emori, V. E., Forest, C., Gleckler, P., Guilyardi, E., Jakob, C., Kattsov, V., Reason, C., and Rummukainen, M.: Evaluation of Climate Models, Climate Change 2013: The Physical Science Basis. Contribution of Working Group I to the Fifth Assessment Report of the Intergovernmental Panel on Climate Change, 2013.

Freund, R., Wilson, W., and Sa, P.: Statistical modeling of a response variable, Regression Analysis; Academic Press: St. Louis, MI, USA, 1998.

Gao, Y., Zhang, L., Zhang, G., Yan, F., Zhang, S., Sheng, L., Li, J., Wang, M., Wu, S., Fu, J. S., et al.: The climate impact on atmospheric stagnation and capability of stagnation indices in elucidating the haze events over North China Plain and Northeast China, Chemosphere, p. 127335, 2020.

Garrido-Perez, J. M., Ordóñez, C., and García-Herrera, R.: Strong signatures of high-latitude blocks and subtropical ridges in winter PM_{10} over Europe, Atmospheric Environment, 167, 49–60, 2017.

Garrido-Perez, J. M., Ordóñez, C., García-Herrera, R., and Barriopedro, D.: Air stagnation in Europe: spatiotemporal variability and impact on air quality, Science of The Total Environment, 645, 1238–1252, 2018.

https://doi.org/10.5194/wcd-2021-5
Preprint. Discussion started: 27 January 2021

Garrido-Perez, J. M., Ordóñez, C., García-Herrera, R., and Schnell, J. L.: The differing impact of air stagnation on summer ozone across Europe, Atmospheric Environment, 219, 117 062, 2019.

Garrido-Perez, J. M., García-Herrera, R., and Ordóñez, C.: Assessing the value of air stagnation indices to reproduce PM_{10} variability in Europe, Atmospheric Research, 248, 105 258, 2021.

Giannadaki, D., Lelieveld, J., and Pozzer, A.: Implementing the US air quality standard for $PM_{2.5}$ worldwide can prevent millions of premature deaths per year, Environmental Health, 15, 88, 2016.

Gómara, I., Pinto, J. G., Woollings, T., Masato, G., Zurita-Gotor, P., and Rodríguez-Fonseca, B.: Rossby wave-breaking analysis of explosive cyclones in the Euro-Atlantic sector, Quarterly Journal of the Royal Meteorological Society, 140, 738–753, 2014.

Hamburger, T., McMeeking, G., Minikin, A., Birmili, W., Dall'Osto, M., O'Dowd, C., Flentje, H., Henzing, B., Junninen, H., Kristensson, A., et al.: Overview of the synoptic and pollution situation over Europe during the EUCAARI-LONGREX field campaign, Atmospheric Chemistry and Physics, 11, 1065–1082, 2011.

Hersbach, H., Bell, B., Berrisford, P., Hirahara, S., Horányi, A., Muñoz-Sabater, J., Nicolas, J., Peubey, C., Radu, R., Schepers, D., et al.: The ERA5 global reanalysis, Quarterly Journal of the Royal Meteorological Society, 146, 1999–2049, 2020.

Horton, D. E., Diffenbaugh, N. S., et al.: Response of air stagnation frequency to anthropogenically enhanced radiative forcing, Environmental Research Letters, 7, 044 034, 2012.

Horton, D. E., Skinner, C. B., Singh, D., and Diffenbaugh, N. S.: Occurrence and persistence of future atmospheric stagnation events, Nature climate change, 4, 698–703, 2014.

Hoskins, B. J., McIntyre, M. E., and Robertson, A. W.: On the use and significance of isentropic potential vorticity maps, Quarterly Journal of the Royal Meteorological Society, 111, 877–946, 1985.

Huang, Q., Cai, X., Song, Y., and Zhu, T.: Air stagnation in China (1985–2014): climatological mean features and trends., Atmospheric Chemistry & Physics, 17, 2017.

Huang, Q., Cai, X., Wang, J., Song, Y., and Zhu, T.: Climatological study of the Boundary-layer air Stagnation Index for China and its relationship with air pollution, Atmospheric Chemistry and Physics, 18, 7573, 2018.

Jacob, D. J. and Winner, D. A.: Effect of climate change on air quality, Atmospheric environment, 43, 51–63, 2009.

Kanawade, V., Srivastava, A., Ram, K., Asmi, E., Vakkari, V., Soni, V., Varaprasad, V., and Sarangi, C.: What caused severe air pollution episode of November 2016 in New Delhi?, Atmospheric Environment, 222, 117 125, 2020.

Kerr, G. H. and Waugh, D. W.: Connections between summer air pollution and stagnation, Environmental Research Letters, 13, 084 001, 2018.

Kerr, G. H., Waugh, D. W., and Miller, S. M.: Jet Stream-surface tracer relationships: Mechanism and sensitivity to source region, Geophysical Research Letters, 48, e2020GL090 714, 2020a.

Kerr, G. H., Waugh, D. W., Steenrod, S. D., Strode, S. A., and Strahan, S. E.: Surface ozone-meteorology relationships: Spatial variations and the role of the jet stream, Journal of Geophysical Research: Atmospheres, 125, e2020JD032 735, 2020b.

Lee, D., Wang, S.-Y. S., Zhao, L., Kim, H. C., Kim, K., and Yoon, J.-H.: Long-term increase in atmospheric stagnant conditions over northeast Asia and the role of greenhouse gases-driven warming, Atmospheric Environment, 241, 117 772, 2020.

Leibensperger, E. M., Mickley, L. J., and Jacob, D. J.: Sensitivity of US air quality to mid-latitude cyclone frequency and implications of 1980–2006 climate change, Atmospheric Chemistry and Physics, 2008.

Leung, D. M., Mickley, L. J., van Donkelaar, A., Shen, L., Martin, R. V., et al.: Synoptic meteorological modes of variability for fine particulate matter ($PM_{2.5}$) air quality in major metropolitan regions of China, Atmospheric Chemistry and Physics, 18, 6733–6748, 2018.

https://doi.org/10.5194/wcd-2021-5
Preprint. Discussion started: 27 January 2021

Leung, L. R. and Gustafson Jr, W. I.: Potential regional climate change and implications to US air quality, Geophysical Research Letters, 32, 2005.

Liao, T., Gui, K., Jiang, W., Wang, S., Wang, B., Zeng, Z., Che, H., Wang, Y., and Sun, Y.: Air stagnation and its impact on air quality during winter in Sichuan and Chongqing, southwestern China, Science of the Total Environment, 635, 576–585, 2018.

Madonna, E., Li, C., Grams, C. M., and Woollings, T.: The link between eddy-driven jet variability and weather regimes in the North Atlantic-European sector, Quarterly Journal of the Royal Meteorological Society, 143, 2960–2972, 2017.

Maraun, D., Shepherd, T. G., Widmann, M., Zappa, G., Walton, D., Gutiérrez, J. M., Hagemann, S., Richter, I., Soares, P. M., Hall, A., et al.: Towards process-informed bias correction of climate change simulations, Nature Climate Change, 7, 764–773, 2017.

Masato, G., Hoskins, B., and Woollings, T. J.: Wave-breaking characteristics of midlatitude blocking, Quarterly Journal of the Royal Meteorological Society, 138, 1285–1296, 2012.

Mickley, L. J., Jacob, D. J., Field, B., and Rind, D.: Effects of future climate change on regional air pollution episodes in the United States, Geophysical Research Letters, 31, 2004.

Molnos, S., Mamdouh, T., Petri, S., Nocke, T., Weinkauf, T., and Coumou, D.: A network-based detection scheme for the jet stream core, Earth System Dynamics, 8, 75–89, 2017.

Montgomery, D. C., Peck, E. A., and Vining, G. G.: Introduction to linear regression analysis, vol. 2, John Wiley & Sons, 2012.

Ordóñez, C., Mathis, H., Furger, M., Henne, S., Hüglin, C., Staehelin, J., and Prévôt, A. S.: Changes of daily surface ozone maxima in Switzerland in all seasons from 1992 to 2002 and discussion of summer 2003, Atmospheric Chemistry and Physics, 5, 1187–1203, 2005.

Ordoñez, C., Barriopedro Cepero, D., García Herrera, R., Sousa, P. M., and Schnell, J. L.: Regional responses of surface ozone in Europe to the location of high-latitude blocks and subtropical ridges, Atmospheric Chemistry and Physics, 17, 3111–3131, 2017.

Ordóñez, C., Barriopedro, D., and García-Herrera, R.: Role of the position of the North Atlantic jet in the variability and odds of extreme PM_{10} in Europe, Atmospheric environment, 210, 35–46, 2019.

Otero, N., Sillmann, J., Schnell, J. L., Rust, H. W., and Butler, T.: Synoptic and meteorological drivers of extreme ozone concentrations over Europe, Environmental Research Letters, 11, 024 005, 2016.

Pope III, C. A., Burnett, R. T., Thun, M. J., Calle, E. E., Krewski, D., Ito, K., and Thurston, G. D.: Lung cancer, cardiopulmonary mortality, and long-term exposure to fine particulate air pollution, JAMA, 287, 1132–1141, 2002.

Prtenjak, M. T., Jeričević, A., Kraljević, L., Bulić, I. H., Nitis, T., and Klaić, Z. B.: Exploring atmospheric boundary layer characteristics in a severe SO2 episode in the north-eastern Adriatic, Atmospheric Chemistry and Physics, 9, 4467–4483, 2009.

Rex, D. F.: Blocking action in the middle troposphere and its effect upon regional climate, Tellus, 2, 275–301, 1950.

Santos, J. A., Pinto, J. G., and Ulbrich, U.: On the development of strong ridge episodes over the eastern North Atlantic, Geophysical Research Letters, 36, 2009.

Scherrer, S. C., Croci-Maspoli, M., Schwierz, C., and Appenzeller, C.: Two-dimensional indices of atmospheric blocking and their statistical relationship with winter climate patterns in the Euro-Atlantic region, International Journal of Climatology: A Journal of the Royal Meteorological Society, 26, 233–249, 2006.

Schnell, J. L. and Prather, M. J.: Co-occurrence of extremes in surface ozone, particulate matter, and temperature over eastern North America, Proceedings of the National Academy of Sciences, 114, 2854–2859, 2017.

Shen, L., Mickley, L., and Tai, A. P.: Influence of synoptic patterns on surface ozone variability over the eastern United States from 1980 to 2012, Atmospheric Chemistry and Physics, 15, 10 925, 2015.

https://doi.org/10.5194/wcd-2021-5
Preprint. Discussion started: 27 January 2021

Sousa, P. M., Trigo, R. M., Barriopedro, D., Soares, P. M., and Santos, J. A.: European temperature responses to blocking and ridge regional patterns, Climate Dynamics, 50, 457–477, 2018.

Sun, W., Hess, P., and Liu, C.: The impact of meteorological persistence on the distribution and extremes of ozone, Geophysical Research Letters, 44, 1545–1553, 2017.

Tai, A. P., Mickley, L. J., and Jacob, D. J.: Correlations between fine particulate matter ($PM_{2.5}$) and meteorological variables in the United States: Implications for the sensitivity of $PM_{2.5}$ to climate change, Atmospheric Environment, 44, 3976–3984, 2010.

Tai, A. P., Mickley, L. J., Jacob, D. J., Leibensperger, E., Zhang, L., Fisher, J. A., and Pye, H.: Meteorological modes of variability for fine particulate matter ($PM_{2.5}$) air quality in the United States: implications for $PM_{2.5}$ sensitivity to climate change, Atmospheric Chemistry and Physics, 12, 3131–3145, 2012.

Taszarek, M., Brooks, H. E., Czernecki, B., Szuster, P., and Fortuniak, K.: Climatological aspects of convective parameters over Europe: a comparison of ERA-interim and sounding data, Journal of Climate, 31, 4281–4308, 2018.

Toro, R., Kvakić, M., Klaić, Z. B., Koračin, D., et al.: Exploring atmospheric stagnation during a severe particulate matter air pollution episode over complex terrain in Santiago, Chile, Environmental pollution, 244, 705–714, 2019.

Valente, R., Imhoff, R., Tanner, R., Meagher, J., Daum, P., Hardesty, R., Banta, R., Alvarez, R., McNider, R., and Gillani, N.: Ozone production during an urban air stagnation episode over Nashville, Tennessee, Journal of Geophysical Research: Atmospheres, 103, 22 555–22 568, 1998.

Vautard, R. and Yiou, P.: Control of recent European surface climate change by atmospheric flow, Geophysical Research Letters, 36, 2009.

Vautard, R., Colette, A., Van Meijgaard, E., Meleux, F., Jan van Oldenborgh, G., Otto, F., Tobin, I., and Yiou, P.: Attribution of wintertime anticyclonic stagnation contributing to air pollution in Western Europe, Bulletin of the American Meteorological Society, 99, S70–S75, 2018.

Wang, J. X. and Angell, J. K.: Air stagnation climatology for the United States, NOAA/Air Resource Laboratory ATLAS, 1999.

Wang, X., Wang, K., and Su, L.: Contribution of atmospheric diffusion conditions to the recent improvement in air quality in China, Scientific reports, 6, 36 404, 2016.

Wang, X., Dickinson, R. E., Su, L., Zhou, C., and Wang, K.: $PM_{2.5}$ pollution in China and how it has been exacerbated by terrain and meteorological conditions, Bulletin of the American Meteorological Society, 99, 105–119, 2018.

Weaver, C., Liang, X.-Z., Zhu, J., Adams, P., Amar, P., Avise, J., Caughey, M., Chen, J., Cohen, R., Cooter, E., et al.: A preliminary synthesis of modeled climate change impacts on US regional ozone concentrations, Bulletin of the American Meteorological Society, 90, 1843–1864, 2009.

Webber, C. P., Dacre, H. F., Collins, W. J., and Masato, G.: The dynamical impact of Rossby wave breaking upon UK PM_{10} concentration, Atmospheric Chemistry and Physics, 17, 867–881, 2017.

Woollings, T., Hannachi, A., and Hoskins, B.: Variability of the North Atlantic eddy-driven jet stream, Quarterly Journal of the Royal Meteorological Society, 136, 856–868, 2010.

Woollings, T., Barriopedro, D., Methven, J., Son, S.-W., Martius, O., Harvey, B., Sillmann, J., Lupo, A. R., and Seneviratne, S.: Blocking and its response to climate change, Current climate change reports, 4, 287–300, 2018.

World Health Organization: Air: when breathing is a threat, https://www.euro.who.int/__data/assets/pdf_file/0011/147656/WHY_Newsletter4.pdf?ua=1, 2011.

Yun, S.-g. and Yoo, C.: The Effects of Spring and Winter Blocking on PM_{10} Concentration in Korea, Atmosphere, 10, 410, 2019.

https://doi.org/10.5194/wcd-2021-5
Preprint. Discussion started: 27 January 2021

Zhang, R., Qiang, L., and RuoNan, Z.: Meteorological conditions for the persistent severe fog and haze event over eastern China in January 2013, Science China Earth Sciences, 57, 26–35, 2014.

Zhang, Y., Ding, A., Mao, H., Nie, W., Zhou, D., Liu, L., Huang, X., and Fu, C.: Impact of synoptic weather patterns and inter-decadal climate variability on air quality in the North China Plain during 1980–2013, Atmospheric environment, 124, 119–128, 2016.